Gettering of Cu by microcavities in bonded/ion-cut silicon-on-insulator and separation by implantation of oxygen

Miao Zhang,[a] Xuchu Zeng, and Paul K. Chu[b]
Department of Physics and Materials Science, City University of Hong Kong, 83 Tat Chee Avenue, Kowloon, Hong Kong

R. Scholz
Max-Planck-Institute of Microstructure Physics, Weinberg 2, D-06120, Halle, Germany

Chenglu Lin
State Key Laboratory of Functional Materials for Informatics, Shanghai Institute of Metallurgy, Chinese Academy of Sciences, Shanghai 200050, People's Republic of China

(Received 28 April 1999; accepted for publication 13 July 1999)

Microcavities formed by H^+ and He^+ implantation and subsequent annealing are effective gettering sites for transition metal impurities in silicon. However, gettering in silicon-on-insulator (SOI) materials is quite different from that in silicon. In this work, we investigate the gettering of Cu to these microcavities in silicon, separation by implantation of oxygen (SIMOX) and bonded/ion-cut SOI wafers. Our data indicate that He^+ implantation in the high dose regime ($0.2-1\times10^{17}\,cm^{-2}$) creates a wide band of microcavities near the projected range without causing blistering on the sample surface. On the other hand, the implantation dose of H^+ needed for stable microcavity formation is relatively narrow ($3-4\times10^{16}\,cm^{-2}$), and this value is related to the projected range. The different behavior of H and He in silicon is discussed and He implantation is more desirable with regard to impurity gettering. Cu is implanted into the surface region of the Si and SOI samples, followed by annealing at 700 and 1000 °C. Our results indicate that the microcavities can effectively getter a high dose of Cu ($2.5\times10^{15}\,cm^{-2}$) at 700 °C in bulk Si wafer, but higher temperature annealing is needed for the effective gettering in SIMOX. Gettering of Cu by the intrinsic defects at or beneath the buried oxide interface of the SIMOX is observed at 700 °C, but no trapped impurities are observed after 1000 °C annealing in the samples in the presence of microcavities. Almost all of the $1\times10^{14}\,cm^{-2}$ Cu implanted into the Si overlayer of the bonded/ion-cut SOI diffuse through the thermally grown oxide layer and are captured by the cavities in the substrate after annealing at 1000 °C. © *1999 American Institute of Physics.* [S0021-8979(99)08920-3]

I. INTRODUCTION

Silicon-on-insulator (SOI) materials have a number of inherent advantages over bulk silicon substrates for high speed, low power complementary metal–oxide–semiconductor (CMOS) integrated circuits, such as immunity to radiation hardness, high speed, and high temperature tolerance.[1,2] SOI thus appears to be the preferred substrate material for ultralarge scale integration (ULSI). Two methods are commonly used to fabricate the SOI materials, namely, separation by implantation of oxygen (SIMOX) and wafer bonding and etch back (BESOI). Recently, the Smart-cut™ process was developed by SOITEC to synthesize high quality SOI wafers.[3] The SIMOX process is quite different from the BESOI and Smart-cut™ processes. The buried oxide (BOX) layer in SIMOX is created by high dose oxygen ion implantation and subsequent high temperature annealing while the BOX layer in BESOI, Smart-cut™ (or more generally referred to as ion-cut) SOI is usually grown thermally. The bond/cut process offers more flexibility as the BOX layer thickness is independent of the thickness of the overlying silicon layer where devices are built.

It is well known that transition metals are detrimental to devices and should be removed from the active region by gettering or other means.[4] In SOI materials, the top Si layer is very thin. This is particularly true for fully depleted metal–oxide–semiconductor (MOS) technology which utilizes the entire overlying silicon film to fabricate devices. Consequently, gettering sites should not be introduced in the overlayer but in the substrate. The gettering processes in SOI wafers are expected to be different from the conventional gettering schemes developed for bulk silicon materials because the impurities have to pass through the BOX layer before reaching the gettering sites.

The increasing use of Cu metallization in the IC industry has spurred intensive research on reducing Cu contamination and how to block Cu diffusion from the metallization to the active IC regions. It has been demonstrated that Cu can diffuse through the BOX layer of SIMOX at elevated temperature.[5–7] However, the BOX layer in BESOI and bonded/ion-cut SOI is much denser than that in SIMOX.

[a]Also affiliated with Shanghai Institute of Metallurgy, People's Republic of China.
[b]Corresponding author; electronic mail: paul.chu@cityu.edu.hk

Gettering of Cu in bonded/ion-cut SOI and BESOI may be more difficult than that in SIMOX. He^+ or H^+ implantation and subsequent annealing can generate empty cavities in silicon,[8–11] and the dangling bonds on the cavity wall can trap impurities by chemisorption thus producing effective gettering sites.[10] Skorupa *et al.* have studied the proximity gettering of Cu to the He implantation induced cavities in SIMOX and revealed that the microcavity band under the BOX in SIMOX traps all of the 1×10^{12} atoms/cm^{-2} Cu after 1000 °C annealing.[13,14] In a separate piece of work, we have demonstrated that a high dose of Cu (4×10^{15} cm^{-2}) can be removed from the Si overlayer and trapped in the cavities in SIMOX.[15]

In order to understand the gettering process and design the optimal experimental protocols, it is very important to study the formation and evolution of the microcavities as well as the related phenomena in H- and He- implanted Si. Some research has been conducted on He^+[8–10] and H^+ implantation[16–19] in Si. The behavior of He and H in silicon is quite different. With the right dose and upon annealing, blisters and flakes readily form on the surface of H-implanted sample but they are much harder to form on He-implanted Si even at a higher implantation dose. The blistering phenomenon is the base of the Smart-cut™[3] and the more general bonded/ion-cut SOI technology, but is undesirable for impurity gettering. However, few studies have been performed to compare the different behavior of H^+- and He^+-implanted silicon. In this comprehensive investigation, channeling Rutherford backscattering spectrometry (RBS) and cross-sectional transmission electron microscopy (XTEM) are employed to compare the microcavity formation and surface morphology during annealing in H^+- and He^+-implanted Si. For the gettering studies, He^+ is implanted into bulk Si, SIMOX and Smartcut™ SOI to compare the characteristics in the three different materials.

II. EXPERIMENT

p-type (100) CZ Si wafers with a resistivity of 20–35 Ω cm were implanted by He^+ ($7-9\times10^{16}$ atoms/cm^2) or H^+ ($3-7\times10^{16}$ atoms/cm^2) at 140 kV at room temperature. The samples were annealed from 300 to 1000 °C for different time duration and examined by RBS, XTEM, and optical microscopy. The channeling RBS measurements were performed using 2 MeV He^+ and the scattering angle was 165°. XTEM was carried out at 200 kV using a Philips CM-20 and JEM400EX.

The SIMOX wafers used in this study were fabricated by implanting 3.3×10^{17} atoms/cm^2 O^+ into *n*-type (100) silicon wafers at 70 kV at 600 °C, followed by annealing at 1300 °C for 6 h in flowing N_2. Afterwards, 5×10^{15} atoms/cm^2 of Cu^+ and 9×10^{16} atoms/cm^2 of He^+ were implanted into the SIMOX at room temperature at 70 and 60 kV, respectively. The room temperature ensured no annealing during Cu and He implantation. As a control for comparison, a *p*-type (100) CZ Si wafer was implanted with Cu^+ and He^+ using conditions similar to the SIMOX wafer. The SIMOX and bulk Si samples were annealed at 700 and 1000 °C for 90 minutes. For the Smart-cut™ SOI provided by SOITEC France, the Si overlayer and BOX were 200 and 400 nm in thickness, respectively. A dose of 9×10^{16} atoms/cm^2 of He^+ was implanted beneath the BOX at 170 kV and 1×10^{14}/cm^2 Cu^+ was implanted into the surface of the Si overlayer. The implanted bonded/ion-cut sample was then annealed at 1000 °C for 3 h. To determine the Cu in-depth distribution in the bulk silicon, SIMOX, and bonded/ion-cut SOI, secondary ion mass spectrometry (SIMS) analysis was performed using a CAMECA IMS-3F ion microanalyzer and a 15 kV O_2^+ primary ion beam.

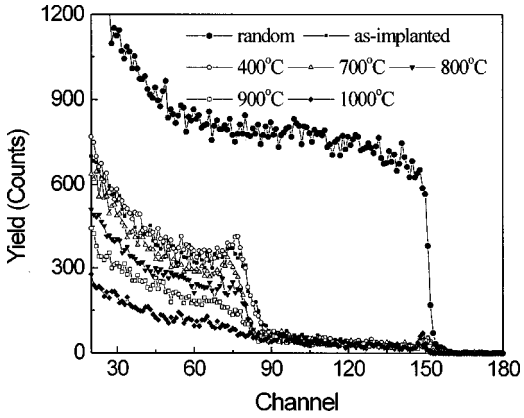

FIG. 1. Channeling RBS spectra of the Si sample implanted with 3×10^{16} atoms/cm^2, 140 kV H^+ and annealed at different temperature for 30 min.

III. RESULTS AND DISCUSSION

We have two objectives, namely, identifying the optimal microcavity gettering process (i.e., either H^+ or He^+ implantation) and investigating/comparing the gettering characteristics in three materials, bulk silicon, SIMOX, and bonded/ion-cut SOI.

Different doses of H^+ in the range of $3-7\times10^{16}$ atoms/cm^2 were implanted into silicon at 140 kV. The samples were then annealed at 300–1000 °C and studied by RBS, XTEM, and optical microscopy. The projected range of 140 kV H^+ simulated by TRIM94 is 120 nm. Figure 1 exhibits the channeling RBS spectra of the 3×10^{16} atoms/cm^2 H^+-implanted Si annealed at different temperatures for 30 min. From the channeling spectrum of the as-implanted sample, it can be seen that there is a damaged layer at a depth corresponding to the projected range of 140 kV H^+. The surface region is still composed of good crystalline silicon. No obvious changes can be observed for the samples annealed at temperature lower than 400 °C. After annealing at above 400 °C, the dechanneling yield begins to diminish, indicating the recovery of the defects, and the number of defects decreases with increasing annealing temperature. No changes are detected at the surface region at all annealing temperature from 300 to 1000 °C. XTEM is performed to observe the microstructure of the 600 °C annealed sample (not shown here), and a slightly damaged layer is observed at the projected range verifying the RBS results, but no bubbles or cavities are found.

Figure 2 displays the XTEM image of the 3.5×10^{16} atoms/cm^2 H^+-implanted sample after 1000 °C an-

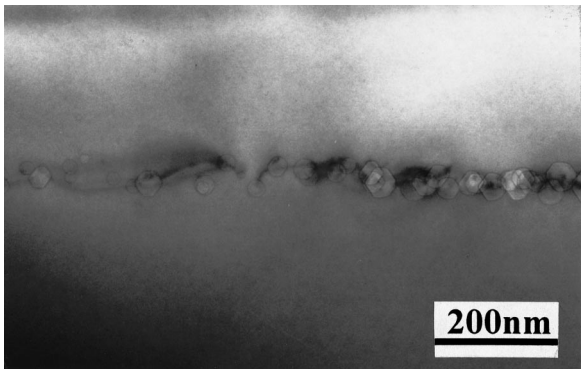

FIG. 2. XTEM image of the 3.5×10^{16} atoms/cm^2, 140 kV H^+-implanted Si followed by 1000 °C, 2 h annealing.

nealing. Microcavities can be observed around the projected range. RBS measurements of the 300–1000 °C samples show similar characteristics as those shown in Fig. 1.

For H^+ implantation doses above 4×10^{16}/cm^2, the RBS results become quite different. Figure 3 shows the RBS spectra acquired from the 5×10^{16} atoms/cm^2 implanted Si. The dechanneling yield in the channeled layer is obviously higher than that in Fig. 1, suggesting that a more heavily damaged layer has formed. However, the surface layer is still of reasonably good crystalline quality. Annealing at 400 °C does not show obvious change at the surface layer, but the dechanneling yield in the channeled layer does increase slightly. The small change may be due to hydrogen released from the defects. When the annealing temperature is over 450 °C, greater changes can be observed on the sample surface by optical spectroscopy or RBS. The spectra in Fig. 3 reveal that the dechanneling yield in the channeled layer in the 450 °C annealed sample increases abruptly to 29%. For comparison, the dechanneling yield of the as-implanted sample is 4%, which is close to that of the perfectly crystalline Si. This sudden increase in the dechanneling yield indicates that the surface layer is substantially altered after 450 °C annealing. A big change is also observed for the 7×10^{16} atoms/cm^2 H^+-implanted Si sample after 400 °C annealing. Under an optical spectroscope, blisters and flaking can be seen on the 5×10^{16}/cm^2 H^+ implanted sample surface, implying local exfoliation has taken place. The degree of blistering and flaking increases with temperature. The

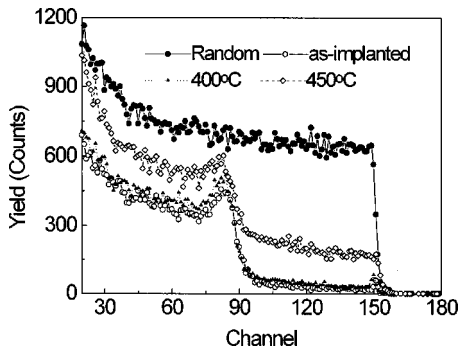

FIG. 3. Channeling RBS results of the Si specimens implanted with 5×10^{16} atoms/cm^2 H^+ at 140 kV before and after annealing at 400 and 450 °C for 30 min.

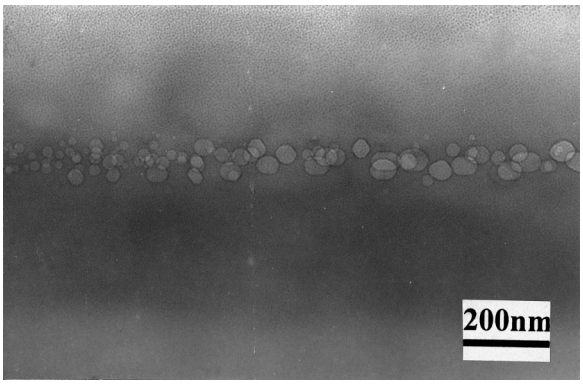

FIG. 4. XTEM image of the 4.5×10^{16} atoms/cm^2, 140 kV H^+-implanted Si after annealing at 900 °C for 2 h showing more microcavities than the sample shown in Fig. 2.

XTEM image of the sample annealed at 900 °C for 2 h depicted in Fig. 4 discloses that the microcavity population is higher than that in the sample shown in Fig. 2 which is implanted with a lower dose. The results indicate that the microcavity density created by H^+ implantation increases with the implantation dose, but a higher H dose will cause serious changes of the surface during the thermal treatment. Figures 5(a) and 5(b) are the XTEM photos of the 4.5×10^{16} atoms/cm^2H^+-implanted Si sample after 1000 °C annealing. A crack can be observed along the projected range [Fig. 5(a)]. Figure 5(b) displays the microcavities and a dark band along the projected range. This dark band contains some {111} and {100} platelets interconnecting with each other. Our study demonstrates that the surface deformation is

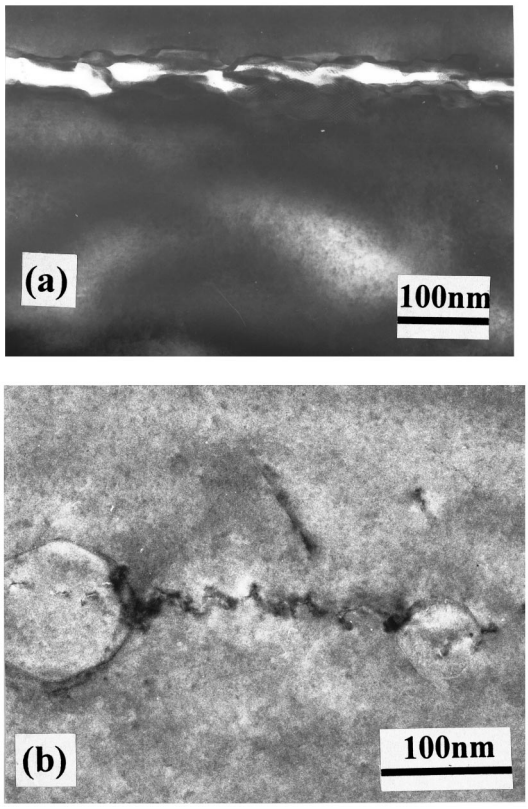

FIG. 5. XTEM image of the 4.5×10^{16} atoms/cm^2, 140 kV H^+-implanted Si after annealing at 1000 °C for 2 h, showing (a) crack at the projected range; (b) cavity with a string of interconnected platelets.

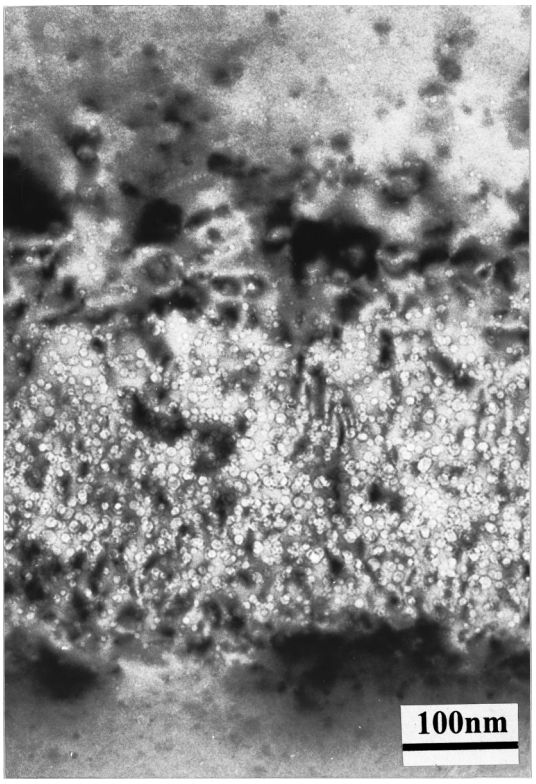

FIG. 6. XTEM image of the 7×10^{16} atoms/cm^2, 140 kV He^+-implanted Si after annealing at 700 °C for 30 min. Dense microcavities have formed in a wide band.

related to the implantation energy. For a Si sample implanted with 5×10^{16} atoms/cm^2 H^+ at 70 kV, blisters are observed on the 400 °C annealed sample.

The formation of the layer with the nanovoids and the annealing behavior of He^+-implanted Si are different from those of the H^+-implanted Si. Figure 6 shows the XTEM image of the 7×10^{16} atoms/cm^2 He-implanted silicon sample after 700 °C annealing. Dense voids as well as strains are present in a 300 nm wide band about the projected range. The channeling RBS spectra of this sample before and after annealing together with a virgin Si wafer (control) are displayed in Fig. 7. The dechanneling yield at the buried damaged layer of the as-implanted sample almost matches that of the random spectrum, indicating that this region is nearly

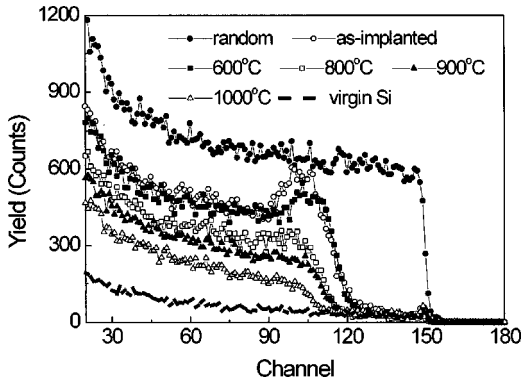

FIG. 7. Channeling RBS spectra of the 7×10^{16} atoms/cm^2, 140 kV He^+-implanted Si after annealing at different temperature for 30 min.

amorphized after high dose He^+ implantation. The RBS results also show that the surface layer above the microcavity band is not deformed during thermal treatments between 300 and 1000 °C. After annealing at 600 °C, the seriously damaged region starts to recover and the number of defects decreases with the increasing temperature. No blisters can be found on the sample surface even after 1000 °C annealing.

We attribute the difference of the annealing behavior between the H^+- and He^+-implanted sample to the different chemical activities of H and He in Si. After implantation, the amount of H present near the projected range far exceeds the solubility limit and may be trapped by the implantation-induced defects. Upon annealing, H is released out from the H-defect complexes. Since H is of high reactivity, it can break the Si–Si bond at the low energy planes of (111), (110), and (100), forming (111), (110), and (100) platelets. It has been reported that Si–H on (111) plane is very stable.[20] However, only (111) and (100) platelets are observed in this study and the reason is not clear. In the meantime, some H may agglomerate to the vacancy clusters and form small bubbles. If the H implantation dose is high enough, the small platelets may connect with each other. The gas pressure in the interconnected platelets makes the sample cleave along the projected range parallel to the sample surface. The typical dimension of a local blister is about 20 μm and about three orders of magnitude larger that of the platelet. If the density of the platelets and bubbles is not high enough to connect each other and cause cleavage at elevated temperatures, the H will diffuse out rapidly.[17] The observed microcavities observed in Figs. 2, 4, and 5 probably originate from the coalescence of empty platelets and voids to reduce the surface energy. On the other hand, He is an inert gas and cannot bond to the silicon. The implanted He in the as-implanted Si agglomerates to the vacancy clusters and forms small bubbles.[21] Upon annealing above 700 °C, the He gas is released leaving behind the microcavities.[22,23] These small cavities will, however, coalesce at elevated temperature. The size of the cavities increases with temperature higher than 700 °C. Based on the observation that blisters do not appear on the Si surface containing dense He bubbles but on the H^+-implanted sample containing interconnected platelets and few bubbles, it is reasonable to conclude that the formation of platelets in the H^+-implanted Si is the key factor for surface deformation and exfoliation.

From the viewpoint of microcavity gettering, He implantation is apparently more favorable because dense cavities can be formed in a large dose range without sample delamination. For our gettering studies, 5×10^{15} atoms/cm^2 Cu^+ and 9×10^{16} atoms/cm^2 He^+ are implanted into a bulk Si wafer at 70 and 60 kV, respectively. The projected ranges calculated by TRIM94 for Cu^+ and He^+ are 50 nm and 500 nm, respectively. After annealing at 700 °C for 2 h, a very large amount of Cu (2.5×10^{15}/cm^2) is trapped in the microcavity band [Fig. 8(a)]. This result demonstrates that the gettering efficiency of the microcavities is very high.

In order to compare the gettering effects of Cu to the voids in Si with those in SOI, a SIMOX wafer is implanted with Cu^+ and He^+ using the same conditions. In the as-implanted SIMOX specimen, the Cu impurities are intro-

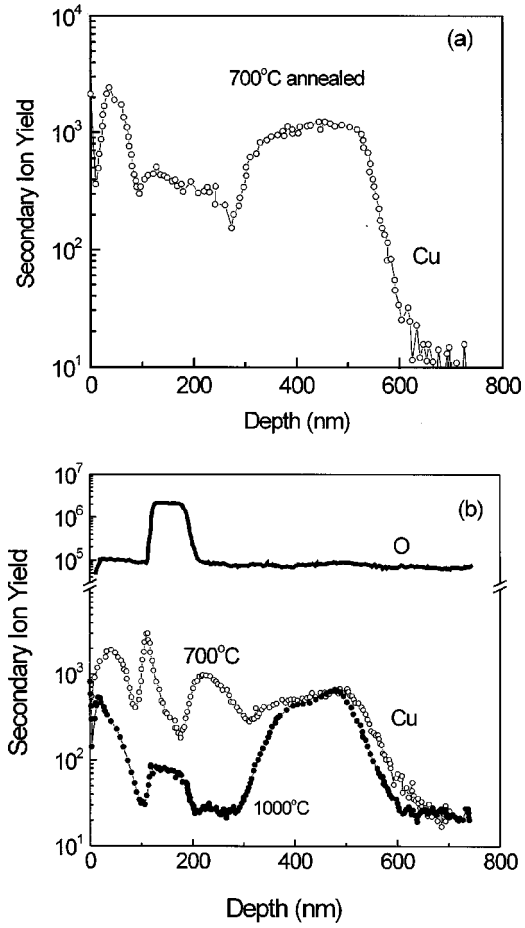

FIG. 8. SIMS results of Cu gettering to the He^+-implantation and annealing induced cavities: (a) in the bulk Si wafer after annealing at 700 °C for 90 min, (b) in the SIMOX wafer after annealing at 700 and 1000 °C for 90 min.

duced into the top Si layer whereas the cavity band is created beneath the BOX layer. Thus, the impurity source and gettering sites are separated by the oxide layer. The Cu distributions after annealing at 700 and 1000 °C are illustrated in Fig. 8(b). After 700 °C annealing, Cu diffuses from the surface and redistributes in three regions: about 1.4×10^{15} atoms/cm^2 remaining in the top Si layer, 2×10^{15} atoms/cm^2 precipitating at the two BOX interfaces, and 1.6×10^{15} atoms/cm^2 being gettered by the microcavity band. For the 1000 °C annealed sample, the amount of Cu trapped by the voids increases to 4×10^{15} atoms/cm^2. A small amount of Cu is found in the BOX layer, but no Cu is detected at the BOX interfaces. This probably indicates that gettering by the intrinsic defects in the BOX is not stable and impurities are released at elevated temperature. The ''surface'' or areal density of trapped sites on the cavity walls after 1000 °C annealing is calculated to be 3.5×10^{15} atoms/cm^2 with an uncertainty of 20%.[15] This value is close to the amount of trapped Cu. No silicide phase is observed in the cavities by XTEM in this study and atomic copper on the cavity walls cannot be directly measured by XTEM. However, our previous work has demonstrated that Cu precipitate indeed form in the cavities when the amount of trapped Cu exceeds the number of trapping sites.[24] Comparing the bulk Si with SIMOX after 700 °C annealing, the amount of Cu trapped in the microcavity band in SIMOX is much less than that in bulk Si. This is due to the gettering of the intrinsic defects at the BOX interfaces in SIMOX. During annealing, Cu has to diffuse through the BOX layer and a portion of that is captured at the BOX interfaces. At a higher temperature, Cu gettered by the BOX defects is released and diffuses to the more stable gettering sites underneath the BOX and trapped by the cavity walls.

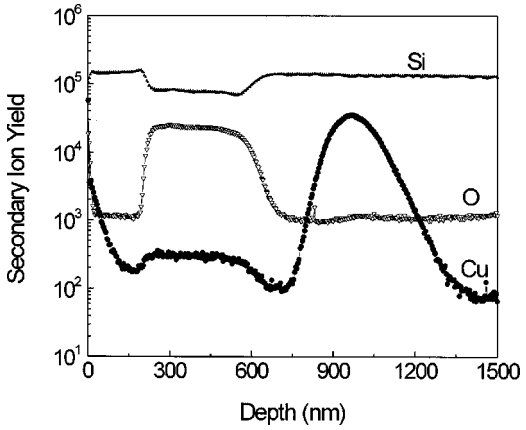

FIG. 9. SIMS profile showing Cu gettering to the microcavities in the bonded/ion-cut SOI wafer after annealing at 1000 °C for 3 h.

Kononchuk, *et al.* have compared the diffusion of Fe implanted into the BOX layer of SIMOX and BESOI and found that Fe diffusion in the BOX of SIMOX is much faster than that in BESOI.[25] Furthermore, they have observed that after annealing, the Fe impurities originally implanted into the BOX are trapped by the intrinsic defects below the BOX of SIMOX, while no Fe is segregated at or below the BOX in BESOI. The BOX layer of bonded/ion-cut SOI is also grown by thermal oxidation, and so there are no intrinsic impurity gettering sites beneath the BOX as well. External gettering sites should be introduced to remove the impurities in bonded/ion-cut SOI. In this study, 9×10^{16} atoms/cm^2 He^+ is implanted into the substrate at 170 kV to generate extrinsic gettering sites. A dose of 1×10^{14} atoms/cm^2 Cu^+ is implanted into the surface of the Si overlayer. After annealing at 1000 °C for 3 h, the Cu in-depth distribution in the bonded/ion-cut SOI is measured by SIMS. As shown in Fig. 9, almost all of the originally implanted Cu 96% is found at the microcavity band, demonstrating that Cu can readily diffuse through the buried thermal oxide layer at elevated temperature and be gettered by the cavities. No Cu pileup is observed at the interfaces of the BOX.

IV. CONCLUSION

The annealing behavior of H^+- and He^+-implanted Si is investigated. It is found that high dose He^+ implantation can generate a wide microcavity band at the projected range without splitting the Si after annealing, while the H^+ implantation dose range required to form microcavities without surface exfoliation is narrower. In our experiments, microcavities are not observed when the H dose is lower than 3×10^{16} atoms/cm^{-2}, but on the other hand, the Si surface will be deformed during annealing if the H dose is higher than

4×10^{15} atoms/cm^2. The XTEM observation demonstrate that the cracking of the H^+-implanted silicon is caused by the interaction of H with Si dangling bonds and breakage of the Si–Si bond forming (111) and (110) platelets. The use of He^+ implantation to form gettering microcavities is therefore preferred. Comparing the Cu gettering process in bulk Si and SIMOX, the latter one is more complex, and a higher annealing temperature is needed for Cu to diffuse through the BOX. The intrinsic defects at the BOX interfaces of SIMOX also act as gettering sites for Cu, but at higher temperature, Cu is released and finally, gettered by the more effective and stable gettering sites formed by the microcavities. Our results demonstrate that microcavity gettering is also effective for bonded/ion-cut SOI such as Smart-cut™ wafers containing a dense buried thermal oxide layer. Almost all of the implanted Cu in the top silicon layer diffuses through the BOX layer and is captured by the microcavity band after annealing at 1000 °C for 3 h (Fig. 9). Thus, microcavity gettering by means of He^+-implantation is suitable for bonded/ion-cut SOI and SIMOX in addition to bulk silicon.

ACKNOWLEDGMENTS

The work was supported by Hong Kong Research Grants Council Earmarked Grant Nos. 9040332 and 9040344, City University of Hong Kong Strategic Research Grant 7000964, and Shanghai Youth Foundation under Grant No. 98QE14028. The authors also acknowledge SOITEC France for providing the Smart-cut™ SOI wafers.

[1] P. N. Dunn, Solid State Technol. **36**, 32 (1990).
[2] J. P. Collinge, *Silicon-on-Insulator Technology*, *Materials to VLSI* (Kluwer Academic, Boston, 1991).
[3] M. Bruel, Electron. Lett. **31**, 1201 (1995).
[4] K. Honda, A. Ohsawa, and N. Toyokura, Appl. Phys. Lett. **46**, 582 (1985).
[5] T. I. Kamins and S. Y. Chiang, J. Appl. Phys. **58**, 2559 (1985).
[6] M. Delfino, M. Jaczynski, A. E. Morgan, C. Vorst, M. E. Lunnon, and P. Maillot, J. Electrochem. Soc. **134**, 2027 (1987).
[7] J. Jabloski, Y. Miyamura, M. Imai, and H. Tsuya, J. Electrochem. Soc. **142**, 2059 (1995).
[8] C. C. Grriffioen, J. H. Evens, P. C. DeJong, and A. Van Veen, Nucl. Instrum. Methods Phys. Res. B **27**, 417 (1987).
[9] S. M. Myers, D. M. Follstaedt, and D. M. Bishop, Mater. Res. Soc. Symp. Proc. **316**, 33 (1994).
[10] D. M. Follstaed, S. M. Myers, G. A. Petersen, and J. W. Medernach, J. Electron. Mater. **25**, 151 (1996).
[11] B. Mohadjeri, J. S. Williams, and J. Wong-Leung, Appl. Phys. Lett. **66**, 1889 (1995).
[12] J. Wong-Leung, C. E. Ascheron, M. Petravic, R. G. Wlliman, and J. S. Williams, Appl. Phys. Lett. **66**, 1231 (1995).
[13] W. Skorupa, N. Hatzopoulos, R. A. Yankov, and A. B. Danilin, Appl. Phys. Lett. **67**, 2992 (1995).
[14] R. A. Yankov, N. Hatzopoulos, W. Skorupa, and A. B. Danilin, Nucl. Instrum. Methods Phys. Res. B **120**, 60 (1996).
[15] M. Zhang, C. Lin, X. Duo, Z. Lin, and Z. Zhou, J. Appl. Phys. **85**, 94 (1999).
[16] T. Hara *et al.*, J. Electrochem. Soc. **143**, L166 (1996).
[17] T. Hara *et al.*, J. Electrochem. Soc. **144**, L78 (1996).
[18] M. F. Beaufort, H. Garem, and J. Lepinoux, Philos. Mag. A **69**, 881 (1994).
[19] G. F. Cerofolini, L. Meda, R. Balbonil, F. Corni, S. Frabboni, G. Ottaviani, R. Tonini, M. Anderle, and R. Canteri, Phys. Rev. B **46**, 2061 (1992).
[20] C. G. Van De Walle, Phys. Rev. B **49**, 4579 (1994).
[21] M. Zhang, C. L. Lin, H. M. Weng, R. Scholz, and U. Gosele, Thin Solid Films **333**, 245 (1998).
[22] C. C. Grriffieon, J. H. Evens, P. C. DeJong, and A. Van Veen, Nucl. Instrum. Methods Phys. Res. B **27**, 417 (1987).
[23] P. F. Fichtner, J. R. Kaschny, R. A. Yankov, A. Mucklich, U. Kreißig, and W. Skorupa, Appl. Phys. Lett. **70**, 732 (1997).
[24] M. Zhang, C. L. Lin, P. L. F. Hemment, K. Gutjhr, and U. Gosele, Appl. Phys. Lett. **72**, 830 (1998).
[25] O. Kononchuk, K. G. Korablev, N. Yarykin, and G. A. Rozgonyi, Appl. Phys. Lett. **73**, 1206 (1998).